

Comprehensive Analytical Expressions for Assessing and Maximizing Technical Benefits of Photovoltaics to Distribution Systems

Karar Mahmoud^{ID} and Matti Lehtonen^{ID}

Abstract—The proliferation of photovoltaic (PV) can cause several operational problems in distribution systems. In this paper, comprehensive analytical expressions (CAEs) are proposed for maximizing the technical benefits of multiple PV units to distribution systems considering the uncertainty of PV generation and load profiles. Specifically, the proposed CAEs quantify and optimize the following five vital indices with multiple PV units: 1) active energy losses, 2) reactive losses, 3) voltage deviations, 4) line congestion margin, and 5) voltage stability index. The smart functions of the PV inverter (i.e., reactive power support and active power curtailment) are also incorporated in the CAEs, complying with the revised IEEE 1547:2018 standard. Further, various PV tracking options are considered, including fixed, one-axis, and two-axis trackers. Unlike existing approaches, the CAEs can simultaneously solve the optimal allocation problem of multiple PV units in a direct manner without needing optimization algorithms, iterative processes, or simplifying procedures. The calculated results reveal the high performance of the CAEs in terms of accuracy, flexibility and computational speed while providing further PV planning options. Moreover, CAEs are effectively utilized for two other applications with promising computational performance, i.e., rapid assessment of PV impacts with annual datasets and optimal centralized/decentralized inverter control.

Index Terms—Photovoltaic, analytical expressions, PV trackers, inverter reactive power, power curtailment, technical benefits.

I. INTRODUCTION

DRIVEN by environmental challenges and energy demand growth, electric utilities have followed ambitious strategies to ensure the optimal and secure operation of electrical power systems while utilizing renewable energy sources (RES). In the distribution system level, the penetration of

photovoltaic (PV), which is a promising, flexible and cost-effective RES type, has remarkably gained momentum worldwide [1], [2]. Typically, PV units are connected to distribution systems so that they supply the electricity in parallel with the utility grid, making the system potentially prone to diverse technical problems [3]–[5]. The intermittent generation and the uncertain nature of these distributed PV units are considered challenging for assessing and maximizing the technical benefits to distribution systems. High PV penetrations could have either remarkable benefits or severe negative impacts on the operation of distribution systems.

Common benefits of PV include reducing generation costs, improving the reliability of the grid, alleviating undesirable carbon emissions, and relieving the transmission system capacity. In turn, intermittent PV generation profiles can decline the standard operation of distribution systems by causing diverse technical problems, most importantly undesirable fluctuations and deviations of voltage, high active energy losses, and excessive reactive power losses [6], [7]. Besides, line congestion and voltage stability margins are vital issues to be considered when integrating PV in distribution systems [8]. Such severe technical problems can limit the hosting capacity of PV while lessening the robustness and efficiency of distribution systems. In this regard, the revised IEEE 1547-2018 standard introduces smart functionalities of the interfacing PV inverter, including voltage/var control and optimal active power dispatch [9], [10]. These smart functionalities, if properly employed, can provide wider control actions of the interfacing inverter, allowing to maximize the technical benefits of PV to distribution systems. Subsequently, it will be more beneficial to consider these issues during the planning phase of PV units in distribution systems.

In the literature, several studies were directed to the optimal planning of PV units considering diverse technical aspects in distribution systems. The authors of [11] have formulated a mixed-integer linear optimization model to allocate PV generation for improving the performance of the grid. In [12], a method was proposed for locating and sizing distributed generations so as to enhance the voltage stability margin in distribution systems. In [13], [14], various approaches have been proposed to solve the PV planning model as a nonlinear programming problem considering loss reduction, active power limitation, the reactive power capability of PV inverters, and multiple PV locations. The authors of [15] have incorporated control schemes of PV inverters in the planning model of active distribution systems. In [16], an improved method

Manuscript received September 17, 2020; revised February 10, 2021 and May 20, 2021; accepted July 11, 2021. Date of publication July 15, 2021; date of current version October 21, 2021. This work was supported by the Department of Electrical Engineering and Automation, Aalto University, Finland. Paper no. TSG-01413-2020. (Corresponding author: Karar Mahmoud.)

Karar Mahmoud is with the Department of Electrical Engineering and Automation, Aalto University, 00076 Espoo, Finland, and also with the Department of Electrical Engineering, Aswan University, 81542 Aswan, Egypt (e-mail: karar.mostafa@aalto.fi).

Matti Lehtonen is with the Department of Electrical Engineering and Automation, Aalto University, 00076 Espoo, Finland (e-mail: matti.lehtonen@aalto.fi).

Color versions of one or more figures in this article are available at <https://doi.org/10.1109/TSG.2021.3097508>.

Digital Object Identifier 10.1109/TSG.2021.3097508

was proposed to evaluate PV hosting capacity considering over-voltage risks and uncertainties. The authors of [17] have investigated the fairness of various curtailment schemes of PV in residential distribution systems.

Driven by the recent development of metaheuristic algorithms, various variants were widely utilized for solve planning problem of PV, such as Jaya algorithm [18], artificial bee colony algorithm [19], gravitational search algorithm [20], genetic algorithm [21], and hybrid algorithms [22]. Metaheuristic algorithms are flexible for multi-objective optimization problems without ensuring a globally optimized solution as they may be trapped into a local minima based on the initial random variables and preset parameters. The authors of [23] have proposed a comprehensive optimization model for the RES sizing and siting in distribution systems based on second order conic programming, considering time-varying generations and loads. A novel method to optimally size and site PV solar panels, diesel generators, and batteries has been introduced in [24] to minimize the overall costs and fulfill the load demand. In [25], the neutral voltage rise and neutral current issues have been mitigated in low-voltage networks by an unbalanced allocation strategy of solar PV. The optimal site and size of PV units, as well as smart microgrid components, have been in [26] determined using a multi-objective optimizer considering demand response. In [27], the optimal allocation problem of PV arrays has been solved using a combination of a fuzzy multi-objective algorithm and a metaheuristic algorithm in a distribution system. A stochastic two-stage mixed-integer linear programming model has been introduced in [28] to determine the optimal allocation and timing of RES considering uncertainty. In [29], a method for maximizing the PV hosting capacity in distribution feeders has been proposed by optimally placing new distribution branches with tie-switches. The authors of [30] have proposed a two-stage game-theoretic planning model for PV panels in distribution systems integrated with an energy sharing mechanism. In [31], the optimal penetration PV level in distribution systems has been determined for reducing power losses considering protection coordination. In [32], a new multistage planning model has been proposed for maximizing the RES hosting capacity with minimum costs.

To achieve a more reliable solution for the planning model of PV in distribution systems, different studies were directed to analytical based methods which are facilely implementable, and guarantee the convergence of the PV planning solution [33]. In [34]–[38], different analytical based methods were introduced for solving the optimal PV allocation problem considering the rated conditions of the load demand and the allocated PV units, thereby ignoring intermittent generation and load profiles. Specifically, these analytical based methods adopt a single objective, such as power loss minimization [34]–[36], reactive power minimization [37], and voltage level improvement [38]. The authors of [39] have proposed a novel index to visualize the impact of DG on power losses and a stability index in distribution systems. In [40], a multi-objective index based analytical method was proposed to determine the optimal capacity and power factor of DG to reduce active and reactive power losses in distribution systems.

TABLE I
MAJOR FEATURES OF PROPOSED ANALYTICAL EXPRESSIONS FOR OPTIMAL PV ALLOCATION AND PREVIOUSLY ANALYTICAL APPROACHES

| REF | Objectives | | | | | Mult. | Unce. | SFs | | TOs |
|-----------|------------|----|----|----|----|-------|-------|-----|-----|-----|
| | PL | QL | VD | CM | SI | | | RPS | APC | |
| [34]–[36] | ✓ | - | - | - | - | ✓ | - | ✓ | - | - |
| [37] | - | ✓ | - | - | - | - | - | - | - | - |
| [38] | - | - | ✓ | - | - | - | - | - | - | - |
| [39] | ✓ | - | - | - | - | ✓ | - | - | - | - |
| [40] | ✓ | ✓ | - | - | - | - | - | ✓ | - | - |
| [41] | ✓ | ✓ | ✓ | - | - | - | ✓ | - | - | - |
| Ours | ✓ | ✓ | ✓ | ✓ | ✓ | ✓ | ✓ | ✓ | ✓ | ✓ |

In [41], several types of voltage-dependent load models were introduced to calculate the optimal penetration of a single PV unit in distribution systems by an analytical expression.

As illustrated above, many state-of-the-art methods have considered advanced aspects of PV planning. However, most analytical based approaches are missing the comprehensive representation of the PV planning model, which is covered in this work. Specifically, analytical based methods follow various simplification procedures for the PV allocation model in distribution systems. In particular, most analytical based methods formulate an analytical expression for allocating a single PV unit, where it is reused for allocating multiple PV units in a sequential manner. This procedure ignores the interaction between the multiple PV units and can lead to non-optimal solutions, besides high computational burden with allocating multiple PVs. Other analytical based methods adopt a single objective or few objectives while ignoring uncertainty of load and PV generation. Most importantly, these analytical based methods do not incorporate the smart functions of PV inverter in their analytical expressions while ignoring the PV tracker options (TOs).

To cover these gaps in the literature, comprehensive analytical expressions (CAEs) are proposed in this paper to effectively solve the PV allocation model in a unified framework. To highlight the contribution of the paper, the major features of the proposed analytical expressions for the optimal PV allocation are compared with the previously analytical based approaches in Table I. The superiority and the unique features of the proposed analytical expressions can be listed as follows.

- The proposed analytical expressions are comprehensive since they involve five indices in distribution systems with multiple PV units, namely active power losses (PL), reactive power losses (QL), voltage deviations (VD), line congestion margin (CM), and voltage stability index (SI);
- The proposed CAEs effectively represent the planning problem of multiple PVs as they are derived in generic matrix forms whose dimensions depend on the number of PV units and the candidate buses. This new unified formulation can express the interaction between the PV units, unlike existing single-PV based formulations.
- Unlike existing methods, the proposed approach proposes a full representation of the uncertainty of PV and load profiles without utilizing average formulae;
- The PV allocation model can be solved directly without requiring iterative or optimization processes;

- The smart functions of the PV inverter (SFs) including, reactive power support (RPS) and active power curtailment (APC) are incorporated in the proposed analytical expressions;
- Different tracking options of PV units are incorporated in the analytical expressions, including fixed, one-axis, and two-axis trackers.

Besides the application of the proposed analytical expressions to the optimal allocation of multiple PV units, they are applied to other important applications in distribution systems interconnected to PVs with predefined capacities, thanks to their light computational burden. Specifically, these applications are the accurate assessment of PV impacts in a short time and proper control of existing PV units. Therefore, the proposed analytical expressions are promising and useful for distribution system operators and planners concerning various topics relating to PV.

II. PROPOSED ANALYTICAL EXPRESSIONS FOR ASSESSING TECHNICAL BENEFITS WITH PVs

In passive distribution systems, loads are normally fed by the main distribution station from which the active power and reactive power flows through distribution lines to load buses. In this work, five indices are considered in distribution systems which are formulated as follows:

$$PL_{B_s} = \sum_{j \in \Omega_B} \frac{R_j}{V_{s,j}^2} (P_{B_{s,j}}^2 + Q_{B_{s,j}}^2), \quad \forall s \in \Psi \quad (1)$$

$$QL_{B_s} = \sum_{j \in \Omega_B} \frac{X_j}{V_{s,j}^2} (P_{B_{s,j}}^2 + Q_{B_{s,j}}^2), \quad \forall s \in \Psi \quad (2)$$

$$VD_{B_s} = \sum_{j \in \Omega_B} \left(\frac{R_j}{V_{s,j}} P_{B_{s,j}} + \frac{X_j}{V_{s,j}} Q_{B_{s,j}} \right)^2, \quad \forall s \in \Psi \quad (3)$$

$$CM_{B_s} = \sum_{j \in \Omega_B} \frac{1}{S_{M_j}^2} (P_{B_{s,j}}^2 + Q_{B_{s,j}}^2), \quad \forall s \in \Psi \quad (4)$$

$$SI_{B_s} = \sum_{j \in \Omega_B} \frac{1}{V_{s,j}^2} (P_{B_{s,j}} R_j + Q_{B_{s,j}} X_j) + \frac{1}{V_{s,j}^4} (P_{B_{s,j}} X_j - Q_{B_{s,j}} R_j)^2, \quad \forall s \in \Psi \quad (5)$$

where PL_{B_s} , QL_{B_s} , VD_{B_s} , CM_{B_s} , and SI_{B_s} represent, respectively, the total active power losses, reactive power losses, voltage deviations, line congestion margin, and voltage stability index at the base case for each state s in the set of states Ψ of the distribution system with a list of buses Ω_B . $P_{B_{s,j}}$ and $Q_{B_{s,j}}$ are the incoming active and reactive power at the base case to bus j for each state s , respectively. $V_{s,j}$ represents voltage magnitude for the state s at the receiving node of the branch j . R_j , X_j , and S_{M_j} are the resistance, the reactance, the nominal power of the branch j , respectively. Detail descriptions and derivations of these indices are given in [37], [42]–[44].

When integrating PV units to the distribution system, the required generated power from the main substation will be decreased due to the contribution of PV. Since the power flow through distribution system lines are affected by PV, the five indices with PV (denoted by PL_{R_s} , QL_{R_s} , VD_{R_s} , CM_{R_s} , and SI_{R_s}) will be significantly changed compared to those at the base case. These updated indices can be expressed by (6)–(10), shown at the bottom of the page, in which

$$\begin{cases} P_{PV_{s,i}} = N_i \times (P_{M_{s,i}} - P_{C_{s,i}}) = N_i \times P_{A_{s,i}} \\ Q_{PV_{s,i}} = P_{PV_{s,i}} L_{s,i}, \quad |Q_{PV_{s,i}}| \leq \sqrt{Z_i^2 - P_{PV_{s,i}}} \end{cases}$$

where $P_{PV_{s,i}}$ and $Q_{PV_{s,i}}$ are the generated active power and reactive power of the PV unit at bus i for state s , respectively. N_i and Z_i represent the number of PV modules and the nominal capacity of the interfacing inverter of PV at bus i , respectively. ζ is a list of valid buses for installing PV. $P_{M_{s,i}}$, $P_{C_{s,i}}$, and $P_{A_{s,i}}$ are the available, the curtailed, and the net active power generation of a PV module at bus i for state s , respectively. $L_{s,i}$ models the relation between active and

$$PL_{PV_s} = \sum_{j \in \Omega_U} \frac{R_j}{V_{s,j}^2} \left[(P_{B_{s,j}} - \sum_{i \in \zeta} \chi_{i,j} P_{PV_{s,i}})^2 + (Q_{B_{s,j}} - \sum_{i \in \zeta} \chi_{i,j} Q_{PV_{s,i}})^2 \right] + \sum_{j \in \Omega_L} \frac{R_j}{V_{s,j}^2} [P_{B_{s,j}}^2 + Q_{B_{s,j}}^2], \quad \forall s \in \Psi \quad (6)$$

$$QL_{PV_s} = \sum_{j \in \Omega_U} \frac{X_j}{V_{s,j}^2} \left[(P_{B_{s,j}} - \sum_{i \in \zeta} \chi_{i,j} P_{PV_{s,i}})^2 + (Q_{B_{s,j}} - \sum_{i \in \zeta} \chi_{i,j} Q_{PV_{s,i}})^2 \right] + \sum_{j \in \Omega_L} \frac{X_j}{V_{s,j}^2} [P_{B_{s,j}}^2 + Q_{B_{s,j}}^2], \quad \forall s \in \Psi \quad (7)$$

$$VD_{PV_s} = \sum_{j \in \Omega_U} \left[\frac{r_j}{V_{s,j}} (P_{B_{s,j}} - \sum_{i \in \zeta} \chi_{i,j} P_{PV_{s,i}}) + \frac{x_j}{V_{s,j}} (Q_{B_{s,j}} - \sum_{i \in \zeta} \chi_{i,j} Q_{PV_{s,i}}) \right]^2 + \sum_{j \in \Omega_L} \left[\frac{r_j}{V_{s,j}} P_{B_{s,j}} + \frac{x_j}{V_{s,j}} Q_{B_{s,j}} \right]^2, \quad \forall s \in \Psi \quad (8)$$

$$CM_{PV_s} = \sum_{j \in \Omega_U} \frac{1}{S_{M_j}^2} ((P_{B_{s,j}} - \sum_{i \in \zeta} \chi_{i,j} P_{PV_{s,i}})^2 + (Q_{B_{s,j}} - \sum_{i \in \zeta} \chi_{i,j} Q_{PV_{s,i}})^2) + \sum_{j \in \Omega_L} \frac{1}{S_{M_j}^2} (P_{B_{s,j}}^2 + Q_{B_{s,j}}^2), \quad \forall s \in \Psi \quad (9)$$

$$SI_{PV_s} = \sum_{j \in \Omega_U} \frac{1}{V_{s,j}^2} \left[R_j (P_{B_{s,j}} - \sum_{i \in \zeta} \chi_{i,j} P_{PV_{s,i}}) + X_j (Q_{B_{s,j}} - \sum_{i \in \zeta} \chi_{i,j} Q_{PV_{s,i}}) \right] + \frac{1}{V_{s,j}^4} \left[X_j (P_{B_{s,j}} - \sum_{i \in \zeta} \chi_{i,j} P_{PV_{s,i}}) - R_j (Q_{B_{s,j}} - \sum_{i \in \zeta} \chi_{i,j} Q_{PV_{s,i}}) \right]^2 + \sum_{j \in \Omega_L} \frac{1}{V_{s,j}^2} [P_{B_{s,j}} R_j + Q_{B_{s,j}} X_j] + \frac{1}{V_{s,j}^4} [P_{B_{s,j}} X_j - Q_{B_{s,j}} R_j]^2, \quad \forall s \in \Psi \quad (10)$$

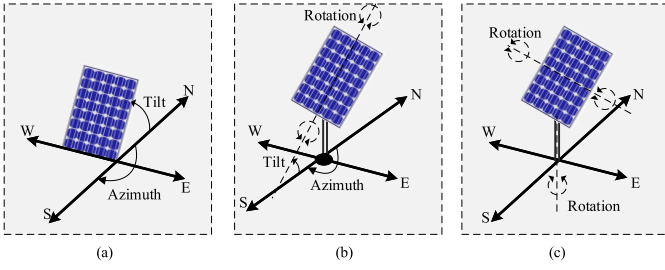


Fig. 1. TOs of PV modules. (a) fixed, (b) one-axis, and (c) two-axis trackers.

reactive power generation according to the PV power factor ($PF_{s,i}$), where $L_{s,i} = \sqrt{1/PF_{s,i}^2 - 1}$. Note that the use of energy storage systems can reduce the total amount of PV power curtailment. This benefit will be achieved by the further flexibility provided by these energy storage systems to charge the surplus PV power at the occasions of high PV generation. Further, the on-load tap changer has a nonlinear mathematical model which makes its implementation to the proposed analytical expressions challenging.

In this work, various TOs of PV units illustrated in Fig. 1 are considered, including fixed, one-axis, and two-axis trackers of PV modules where their detailed mathematical models are given in [45]. Here, we consider the TOs as an input for the PV planning model while it could be a factor to be included in the formulation as in [13], [15]. Note that the first terms of (6)-(10) involve the corresponding indices for the upstream branches (denoted as Ω_U) of PV while the second ones include the corresponding indices for the down-stream branches (denoted as Ω_L) of PV, where $\Omega_U \cup \Omega_L = \Omega_B$. Note that $\chi_{i,j}$ is equal to 1 if bus j is located in the upstream zone of the PV bus i ; otherwise, it is 0. To quantify the PV impacts on the five technical conditions of the distribution system, the following formulae can be utilized:

$$PLI_{PV} = \sum_{s \in \Psi} (PL_{B_s} - PL_{PV_s}) \times Pr(s) \quad (11)$$

$$QLI_{PV} = \sum_{s \in \Psi} (QL_{B_s} - QL_{PV_s}) \times Pr(s) \quad (12)$$

$$VDI_{PV} = \sum_{s \in \Psi} (VD_{B_s} - VD_{PV_s}) \times Pr(s) \quad (13)$$

$$CMI_{PV} = \sum_{s \in \Psi} (CM_{B_s} - CM_{PV_s}) \times Pr(s) \quad (14)$$

$$SII_{PV} = \sum_{s \in \Psi} (SI_{B_s} - SI_{PV_s}) \times Pr(s) \quad (15)$$

where PLI_{PV} , QLI_{PV} , VDI_{PV} , CMI_{PV} , and SII_{PV} are the improvements (i.e., reductions) in total active power losses, reactive power losses, voltage deviations, line congestion margin, and voltage stability index, due to PV, respectively. $Pr(s)$ is the probability of state s . By substituting (1)-(5) and (6)-(10) into (11)-(15), the resulting formulae will be significantly reduced since the summation terms relating to the down-stream branches (Ω_L) will be eliminated due to the subtraction process. These reduced analytical expressions are solved in a direct way without requiring iterative power flow solutions. This low-computational burden allows to rapidly assess the

PV impacts on the various indices with high computational speed, thereby facilitating assessment and allocation problems of multiple PV units. In this work, we focus on the PV installation in medium-voltage distribution systems, which is commonly treated as balanced systems. Note that the investment cost of PVs and reliability indices is not considered in this work and left for a future study.

III. PROPOSED ANALYTICAL EXPRESSIONS FOR OPTIMAL PV SIZING

A. Single-Objective Formulation

Here, we proposed analytical expressions for the optimal sizing of multiple PV units in distribution systems. After substituting (1)-(10) into (11)-(15), the first partial derivative of the five single-function with respect to N_m and L_m are given in Table II, where the PV bus $m \in \zeta$. It is a fact that the critical points of these functions are the points at which the corresponding derivative is zero. Based on this mathematical fact, the following conditions are satisfied at the optimal points of the variables:

$$\begin{cases} \frac{\partial PLI_{PV}}{\partial N_m} = 0, & \frac{\partial PLI_{PV}}{\partial L_m} = 0, & \forall m \in \zeta \\ \frac{\partial QLI_{PV}}{\partial N_m} = 0, & \frac{\partial QLI_{PV}}{\partial L_m} = 0, & \forall m \in \zeta \\ \frac{\partial VDI_{PV}}{\partial N_m} = 0, & \frac{\partial VDI_{PV}}{\partial L_m} = 0, & \forall m \in \zeta \\ \frac{\partial CMI_{PV}}{\partial N_m} = 0, & \frac{\partial CMI_{PV}}{\partial L_m} = 0, & \forall m \in \zeta \\ \frac{\partial SII_{PV}}{\partial N_m} = 0, & \frac{\partial SII_{PV}}{\partial L_m} = 0, & \forall m \in \zeta \end{cases} \quad (16)$$

These 10 partial derivatives summarized in Table II can be written for each PV unit in the distribution system. For each index, two linear systems of equations for module numbers and power factors of all PV units can be constructed, whose lengths are equal to the number of PV units. These linear systems of equations for each index can be rearranged in generic matrix forms expressed by (17) and (18).

$$\begin{bmatrix} N_1 \\ \vdots \\ N_{U-1} \\ N_U \end{bmatrix} = \begin{bmatrix} A_{1,1} & \dots & A_{1,U-1} & A_{1,U} \\ \vdots & \ddots & \vdots & \vdots \\ A_{U-1,1} & \dots & A_{U-1,U-1} & A_{U-1,U} \\ A_{U,1} & \dots & A_{U,U-1} & A_{U,U} \end{bmatrix}^{-1} \begin{bmatrix} B_1 \\ \vdots \\ B_{U-1} \\ B_U \end{bmatrix} \quad (17)$$

$$\begin{bmatrix} L_1 \\ \vdots \\ L_{U-1} \\ L_U \end{bmatrix} = \begin{bmatrix} C_{1,1} & \dots & C_{1,U-1} & C_{1,U} \\ \vdots & \ddots & \vdots & \vdots \\ C_{U-1,1} & \dots & C_{U-1,U-1} & C_{U-1,U} \\ C_{U,1} & \dots & C_{U,U-1} & C_{U,U} \end{bmatrix}^{-1} \begin{bmatrix} D_1 \\ \vdots \\ D_{U-1} \\ D_U \end{bmatrix} \quad (18)$$

where generic formulae of the elements of **A**, **B**, **C**, and **D** matrices for the five single-objectives are summarized in Tables III–IV. U represents the number of PV units distributed among valid buses in the distribution system. Note that the subscripts m and n represent the corresponding PV bus buses. The subscripts m represents the PV bus in which the corresponding optimality conditions expressed by (17) are satisfied. However, the subscript i represents an index of any bus belonging to the list of PV buses.

Note that the planning model of PV is modeled in this work as a convex optimization problem, as formulated in

TABLE II
DERIVATIVES OF PLI_R , QLI_R , VDI_R , CMI_R , AND SIH_R WITH RESPECT TO N_m AND D_m

| | |
|--|--|
| $\frac{\partial PLIPV}{\partial N_m}$ | $2 \sum_{s \in \Psi} \sum_{j \in \Omega_U} x_{m,j} P_{A_{s,m}} \frac{R_j}{\sqrt{2}} \left[(P_{B_{s,j}} - \sum_{i \in \zeta} x_{i,j} N_i \times P_{A_{s,i}}) + L_{s,m} (Q_{B_{s,j}} - \sum_{i \in \zeta} x_{i,j} N_i \times P_{A_{s,i}} L_{s,i}) \right] \times Pr(s)$ |
| $\frac{\partial QLIPV}{\partial N_m}$ | $2 \sum_{s \in \Psi} \sum_{j \in \Omega_U} x_{m,j} P_{A_{s,m}} \frac{X_j}{\sqrt{2}} \left[(P_{B_{s,j}} - \sum_{i \in \zeta} x_{i,j} N_i \times P_{A_{s,i}}) + L_{s,m} (Q_{B_{s,j}} - \sum_{i \in \zeta} x_{i,j} N_i \times P_{A_{s,i}} L_{s,i}) \right] \times Pr(s)$ |
| $\frac{\partial VDI PV}{\partial N_m}$ | $2 \sum_{s \in \Psi} \sum_{j \in \Omega_U} x_{m,j} P_{A_{s,m}} \left[\frac{r_j}{\sqrt{2}} (P_{B_{s,j}} - \sum_{i \in \zeta} x_{i,j} N_i \times P_{A_{s,i}}) + \frac{x_j}{\sqrt{2}} (Q_{B_{s,j}} - \sum_{i \in \zeta} x_{i,j} N_i \times P_{A_{s,i}} L_{s,i}) \right] \left[\frac{R_j}{\sqrt{2}} + \frac{X_j}{\sqrt{2}} L_{s,m} \right] \times Pr(s)$ |
| $\frac{\partial CMI PV}{\partial N_m}$ | $2 \sum_{s \in \Psi} \sum_{j \in \Omega_U} x_{m,j} P_{A_{s,m}} \frac{1}{S_{M,j}^2} \left[(P_{B_{s,j}} - \sum_{i \in \zeta} x_{i,j} N_i \times P_{A_{s,i}}) + L_{s,m} (Q_{B_{s,j}} - \sum_{i \in \zeta} x_{i,j} N_i \times P_{A_{s,i}} L_{s,i}) \right] \times Pr(s)$ |
| $\frac{\partial SIH PV}{\partial N_m}$ | $\sum_{s \in \Psi} \sum_{j \in \Omega_U} x_{m,j} P_{A_{s,m}} \frac{1}{\sqrt{2}} \left[R_j + X_j L_{s,m} + 2 \frac{1}{\sqrt{2}} \left[X_j + R_j L_{s,m} \right] \times \left[X_j (P_{B_{s,j}} - \sum_{i \in \zeta} x_{i,j} N_i \times P_{A_{s,i}}) + R_j (Q_{B_{s,j}} - \sum_{i \in \zeta} x_{i,j} N_i \times P_{A_{s,i}} L_{s,i}) \right] \right] \times Pr(s)$ |
| $\frac{\partial PLIPV}{\partial L_m}$ | $2 \sum_{s \in \Psi} \sum_{j \in \Omega_U} x_{m,j} P_{A_{s,m}} N_m \frac{R_j}{\sqrt{2}} \left[(Q_{B_{s,j}} - \sum_{i \in \zeta} x_{i,j} N_i \times P_{A_{s,i}} L_{s,i}) \right] \times Pr(s)$ |
| $\frac{\partial QLIPV}{\partial L_m}$ | $2 \sum_{s \in \Psi} \sum_{j \in \Omega_U} x_{m,j} P_{A_{s,m}} N_m \frac{X_j}{\sqrt{2}} \left[(Q_{B_{s,j}} - \sum_{i \in \zeta} x_{i,j} N_i \times P_{A_{s,i}} L_{s,i}) \right] \times Pr(s)$ |
| $\frac{\partial VDI PV}{\partial L_m}$ | $2 \sum_{s \in \Psi} \sum_{j \in \Omega_U} x_{m,j} P_{A_{s,m}} N_m \left[\frac{r_j}{\sqrt{2}} (P_{B_{s,j}} - \sum_{i \in \zeta} x_{i,j} N_i \times P_{A_{s,i}}) + \frac{x_j}{\sqrt{2}} (Q_{B_{s,j}} - \sum_{i \in \zeta} x_{i,j} N_i \times P_{A_{s,i}} L_{s,i}) \right] \left[\frac{X_j}{\sqrt{2}} \right] \times Pr(s)$ |
| $\frac{\partial CMI PV}{\partial L_m}$ | $2 \sum_{s \in \Psi} \sum_{j \in \Omega_U} x_{m,j} P_{A_{s,m}} N_m \frac{1}{S_{M,j}^2} \left[(Q_{B_{s,j}} - \sum_{i \in \zeta} x_{i,j} N_i \times P_{A_{s,i}} L_{s,i}) \right] \times Pr(s)$ |
| $\frac{\partial SIH PV}{\partial L_m}$ | $\sum_{s \in \Psi} \sum_{j \in \Omega_U} x_{m,j} P_{A_{s,m}} \frac{1}{\sqrt{2}} \left[X_j + 2 \frac{1}{\sqrt{2}} \left[R_j \right] \times \left[X_j (P_{B_{s,j}} - \sum_{i \in \zeta} x_{i,j} N_i \times P_{A_{s,i}}) + R_j (Q_{B_{s,j}} - \sum_{i \in \zeta} x_{i,j} N_i \times P_{A_{s,i}} L_{s,i}) \right] \right] \times Pr(s)$ |

the quadratic objective functions (6)-(10) and (11)-(15). As a result, these quadratic objective functions are differentiated expressions that can be solved directly. Regarding analytical expressions (17) and (18), it is important to note that they can be solved directly even with placing more than 1 PV unit without requiring an iterative non-linear algebraic equation solver. This feature can be justified since all elements of **A**, **B**, **C**, and **D** for all the five single-objectives (given in Tables III and IV) are a function given parameters or computed variables at the initial stage.

B. Multi-Objective Formulation

Practically, the PV allocation problem is formulated as a multi-objective function considering conflicting single-objectives. Here, the proposed planning model of PV considers 5 different single-objectives, which quantify PL, QL, VD, CM, and SI to be minimized. The merit of this multi-objective formulation is enabling to adjust and investigate the trade-off between the different single-objective functions, and so, wider PV planning options are available. To assign the most promising optimal solution of this multi-objective optimization model, we adopt the weighted sum method. Specifically, the five single-objective functions (1)-(5) are expressed into a single objective function (f_B) by adopting weightings, which can be written as follows:

$$f_B = \sum_{s \in S} \left(\frac{WF_1}{PL_0} \times PL_{B_s} + \frac{WF_2}{QL_0} \times QL_{B_s} + \frac{WF_3}{VD_0} \times VD_{B_s} + \frac{WF_4}{CM_0} \times CM_{B_s} + \frac{WF_5}{SI_0} \times SI_{B_s} \right) \times Pr(s) \quad (19)$$

where WF_1 , WF_2 , WF_3 , WF_4 , and WF_5 are weights of PL_{B_s} , QL_{B_s} , VD_{B_s} , CM_{B_s} , and SI_{B_s} , respectively. PL_0 , QL_0 , VD_0 , CM_0 , and SI_0 are the corresponding normalizing factors, respectively. Note that the sum of the five weighting factors

(WF_1 , WF_2 , WF_3 , WF_4 , and WF_5) equals 1. These weighting factors are incorporated to set the importance of each single-objective function with respect to the other single-objectives. The choice of these weighting factors can be assigned by system planners according to the grid codes and conditions. Regarding PL_0 , QL_0 , VD_0 , CM_0 , and SI_0 values, they are considered here to be equal to the corresponding PL , QL , VD , CM , and SI values at the nominal loading condition in the distribution system under study without PV, respectively.

Similar to f_B , a single objective function (f_{PV}) that considers the five single-objective functions (6)-(10) with PVs can be expressed. Then, the first partial derivatives of f (where $f_I = f_B - f_{PV}$) with respect to N_m and L_m ($\frac{\partial f_I}{\partial N_m}$, $\frac{\partial f_I}{\partial L_m}$) can be formulated. Similar to the derivation of **A**, **B**, **C**, and **D** matrices of each single-objective, the corresponding matrices of f_I is expressed as follows:

$$\begin{aligned} \mathbf{ABCD}_f &= \frac{WF_1}{PL_0} \times \mathbf{ABCD}_{PLI} + \frac{WF_2}{QL_0} \times \mathbf{ABCD}_{QLI} \\ &+ \frac{WF_3}{VD_0} \times \mathbf{ABCD}_{VDI} + \frac{WF_4}{CM_0} \\ &\times \mathbf{ABCD}_{CMI} + \frac{WF_5}{SI_0} \times \mathbf{ABCD}_{SIH} \end{aligned} \quad (20)$$

in which $\mathbf{ABCD} = [\mathbf{A} \ \mathbf{B} \ \mathbf{C} \ \mathbf{D}]^T$.

IV. APPLICATION TO OPTIMAL PV ALLOCATION

In this section, the application of the proposed CAEs to plan PVs in distribution systems is described. Specifically, this planning PV problem involves the determination of the optimal locations, sizes, and numbers of PV units. Fig. 2 show the flowchart of the proposed PV planning model by the CAEs. Below, the solution process of this planning problem through the proposed analytical expressions can be described as follows:

TABLE III
 GENERIC FORMULAE OF **A** AND **B** ELEMENTS FOR DIFFERENT OBJECTIVES

| Obj. | $A_{n,m}$ | $B_{n,m}$ |
|------|---|--|
| PLI | $\sum_{s \in \Psi} \sum_{j \in \Omega} \frac{R_j}{\sqrt{2}} x_{m,j} x_{n,j}$ $P_{A_{s,m}} P_{A_{s,n}} (1 + L_{s,n} L_{s,m}) \times Pr(s)$ | $\sum_{s \in \Psi} \sum_{j \in \Omega} \frac{R_j}{\sqrt{2}} x_{m,j}$ $P_{A_{s,m}} (P_{B_{s,j}} + L_{s,m} Q_{B_{s,j}}) \times Pr(s)$ |
| QLI | $\sum_{s \in \Psi} \sum_{j \in \Omega} \frac{X_j}{\sqrt{2}} x_{m,j} x_{n,j}$ $P_{A_{s,m}} P_{A_{s,n}} (1 + L_{s,n} L_{s,m}) \times Pr(s)$ | $\sum_{s \in \Psi} \sum_{j \in \Omega} \frac{X_j}{\sqrt{2}} x_{m,j}$ $P_{A_{s,m}} (P_{B_{s,j}} + L_{s,m} Q_{B_{s,j}}) \times Pr(s)$ |
| VDI | $\sum_{s \in \Psi} \sum_{j \in \Omega} x_{m,j} x_{n,j} P_{A_{s,m}} P_{A_{s,n}}$ $(\frac{R_j}{\sqrt{2}} + L_{s,m} \frac{X_j}{\sqrt{2}}) (\frac{R_j}{\sqrt{2}} + L_{s,n} \frac{X_j}{\sqrt{2}}) \times Pr(s)$ | $\sum_{s \in \Psi} \sum_{j \in \Omega} x_{m,j} P_{A_{s,m}}$ $(\frac{R_j}{\sqrt{2}} + L_{s,m} \frac{X_j}{\sqrt{2}}) (\frac{R_j}{\sqrt{2}} P_{B_{s,j}} + \frac{X_j}{\sqrt{2}} Q_{B_{s,j}}) \times Pr(s)$ |
| CMI | $\sum_{s \in \Psi} \sum_{j \in \Omega} x_{m,j} x_{n,j} P_{A_{s,m}} P_{A_{s,n}}$ $(\frac{1}{S_{M,j}}) (1 + L_{s,n} L_{s,m}) \times Pr(s)$ | $\sum_{s \in \Psi} \sum_{j \in \Omega} x_{m,j} P_{A_{s,m}}$ $(\frac{1}{S_{M,j}}) (P_{B_{s,j}} + L_{s,m} Q_{B_{s,j}}) \times Pr(s)$ |
| SII | $\sum_{s \in \Psi} \sum_{j \in \Omega} x_{m,j} x_{n,j} P_{A_{s,m}} P_{A_{s,n}}$ $2 \frac{1}{\sqrt{2}} (X_j + R_j L_{s,m}) (X_j + R_j L_{s,n}) \times Pr(s)$ | $\sum_{s \in \Psi} \sum_{j \in \Omega} x_{m,j} P_{A_{s,m}} \left((R_j + X_j L_{s,m}) + \right.$ $\left. 2 \frac{1}{\sqrt{2}} (X_j + R_j L_{s,m}) (X_j P_{B_{s,j}} + R_j Q_{B_{s,j}}) \right) \times Pr(s)$ |

TABLE IV
 GENERIC FORMULAE OF **C** AND **D** ELEMENTS FOR DIFFERENT OBJECTIVES

| Obj. | $C_{n,m}$ | $D_{n,m}$ |
|------|--|---|
| PLI | $\sum_{s \in \Psi} \sum_{j \in \Omega} x_{m,j} x_{n,j} \frac{R_j}{\sqrt{2}} P_{PV_{s,m}} P_{PV_{s,n}} \times Pr(s)$ | $\sum_{s \in \Psi} \sum_{j \in \Omega} \frac{R_j}{\sqrt{2}} x_{m,j} P_{PV_{s,m}} Q_{B_{s,j}} \times Pr(s)$ |
| QLI | $\sum_{s \in \Psi} \sum_{j \in \Omega} x_{m,j} x_{n,j} \frac{X_j}{\sqrt{2}} P_{PV_{s,m}} P_{PV_{s,n}} \times Pr(s)$ | $\sum_{s \in \Psi} \sum_{j \in \Omega} \frac{X_j}{\sqrt{2}} x_{m,j} P_{PV_{s,m}} Q_{B_{s,j}} \times Pr(s)$ |
| VDI | $\sum_{s \in \Psi} \sum_{j \in \Omega} x_{m,j} x_{n,j} \frac{X_j}{\sqrt{2}} P_{PV_{s,m}} P_{PV_{s,n}} \times Pr(s)$ | $\sum_{s \in \Psi} \sum_{j \in \Omega} x_{m,j} \frac{X_j}{\sqrt{2}} P_{PV_{s,m}} (\frac{R_j}{\sqrt{2}} P_{B_{s,j}}$ $+ \frac{X_j}{\sqrt{2}} Q_{B_{s,j}} - \frac{R_j}{\sqrt{2}} \sum_{i \in \zeta} x_{i,j} P_{R_{s,i}}) \times Pr(s)$ |
| CMI | $\sum_{s \in \Psi} \sum_{j \in \Omega} x_{m,j} x_{n,j} \frac{1}{S_{M,j}} P_{PV_{s,m}} P_{PV_{s,n}} \times Pr(s)$ | $\sum_{s \in \Psi} \sum_{j \in \Omega} x_{m,j} \frac{1}{S_{M,j}} P_{PV_{s,m}} Q_{B_{s,j}} \times Pr(s)$ |
| SII | $\sum_{s \in \Psi} \sum_{j \in \Omega} x_{m,j} x_{n,j} \frac{2R_j^2}{\sqrt{2}} P_{PV_{s,m}} P_{PV_{s,n}} \times Pr(s)$ | $\sum_{s \in \Psi} \sum_{j \in \Omega} x_{m,j} \frac{1}{\sqrt{2}} P_{PV_{s,m}} (X_j + \frac{2R_j}{\sqrt{2}}$ $(X_j P_{B_{s,j}} - X_j \sum_{i \in \zeta} x_{i,j} P_{PV_{s,i}} + R_j Q_{B_{s,j}}) \times Pr(s)$ |

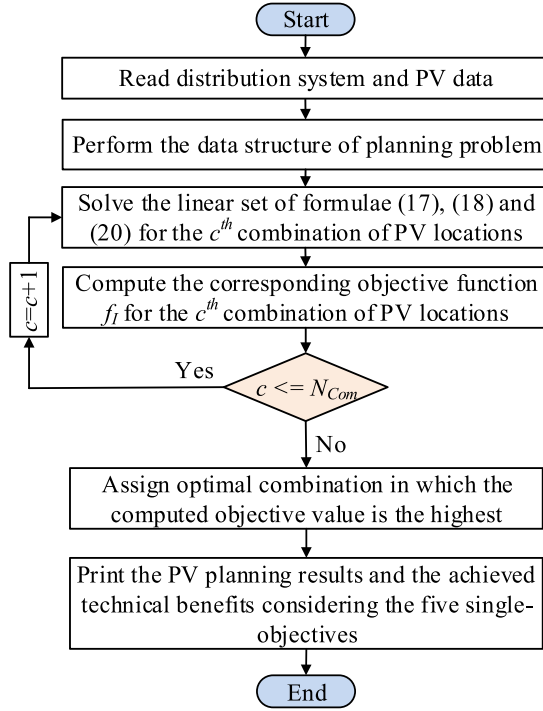


Fig. 2. Flowchart of the proposed planning method of PV by the CAEs.

- 1) Read full data of the distribution system under study, involving parameters of branches and historical profiles of loads. Regarding PV units, their data are also read,

including PV parameters, historical dataset of environmental conditions, and candidate locations for each PV unit. Further, the upper and lower capacity limits of each PV unit and the total PV in the distribution system are required, besides the adopted active power curtailment and reactive power inverter settings.

- 2) Perform the data structure of the distribution system, and build a combined probability model of PV generation and loads based on [12]. Run power flow at discrete load levels, and save the corresponding power flow results including voltages of buses, and active/reactive power flows through branches. Performing the data structure aims to construct all required vectors, such as $P_{B_{s,j}}$ and $Q_{B_{s,j}}$ at the base case to bus j for each state s . Further, the active power generation of the PV module at various states is computed in this step.
- 3) Construct the matrix χ considering all possible combinations of PV locations whose number is denoted by N_{Com} .
- 4) Compute the optimal sizes of multiple PVs for all possible combinations of sites using (17) and (18) considering **A**, **B**, **C**, and **D** matrices computed by (20), and save the corresponding objective f . Then, determine the best combination of locations and sizes of PV units in which the computed objective value is the highest.
- 5) Print the optimal locations and sizes of PV units, besides the values of indices.

Note that the proposed PV planning method considers all possible combinations of locations for the PVs for single PV

allocation. However, a strategy can be used to shorten the number of possible combinations of locations for the PVs in the case of multiple PV allocation. This strategy involves the assignment of the top candidate buses in each lateral of the distribution system. The list of these top candidate buses is identified based on their corresponding technical benefits estimated by the proposed analytical expressions.

Driven by the high computational performance of the proposed direct CAEs, they are also applicable to two other applications which are the PV assessment and the PV inverter control. This feature gives the proposed CAEs superiority against existing approaches that utilize optimization algorithms with a high computational burden.

V. RESULTS AND DISCUSSION

A. Test System and Dataset

The proposed method was tested using the IEEE 33-bus distribution system described in [35]. All busses of the test system (except the slack bus) are assumed as candidate locations for PVs while it is supposed that the system planner aims to optimally allocate up to six PV units in different buses. A dataset of load and solar radiation for three years with one-hour resolution in Finland are utilized to construct the combined probabilistic model. It is demonstrated that the Beta pdf is the most suitable function for modeling solar irradiance of PV while the normal pdf is the most suitable function for modeling the load. Here, the solar irradiance and load demand are considered as discrete datasets. Specifically, for each time duration, they are discretized into 10 normalized regions in the range from 0 to 1.0. The mathematical formulation of these probabilistic load and PV models is given in [12]. The proposed formulations were implemented in MATLAB 2019b where comprehensive tests were performed on an Intel Xeon E3-1230 3.40-GHz PC with 16 GB of RAM.

B. PV With Different Trackers

The proposed analytical expressions are applied first to allocate 1, 2, 3, 4, 5, and 6 PV units, operating at unity power factors, with the three different trackers. Here, the weights of all single-objective functions are set to be equal to 0.2. Table V shows the results of the PV allocation in terms of the optimal locations and sizes of PV, and the corresponding values of the objective function f_{PV} and their improvement percentage (f_{IP}) with respect to those of the base case (f_B), computed by $f_{IP} = 100 * f_i / f_B$. Note that the base case represents the scenario when the 33-bus distribution system works without PV units during the studied period while all objectives have equal weights. The corresponding objective function (f_B) value is 0.41 which is much higher than those of the proposed allocation cases (1-6 PV units).

As seen from Table V, the optimal sizes of PV with the 2-axis PV tracker are lower than those with fixed and 1-axis PV trackers while the highest PV sizes are noticed with the fixed system for all numbers of PV units. For instance, the computed PV size when installing one PV unit (i.e., $U = 1$) with fixed and 1-axis PV trackers are 2.14 and 1.98 MW, respectively, while it is only 1.82 MW with 2-axis trackers.

TABLE V
RESULTS OF PV ALLOCATION WITH DIFFERENT TRACKERS BY THE PROPOSED METHOD

| U | Bus | Fixed (open rack) | | 1-Axis Tracking | | | 2-Axis Tracking | | | |
|---|-----|-------------------|----------|-----------------|------|----------|-----------------|------|----------|--------------|
| | | Size | f_{PV} | $f_{IP}(\%)$ | Size | f_{PV} | $f_{IP}(\%)$ | Size | f_{PV} | $f_{IP}(\%)$ |
| 1 | 10 | 2.14 | 0.3484 | 15.01 | 1.98 | 0.3469 | 15.39 | 1.82 | 0.3443 | 16.02 |
| 2 | 10 | 1.64 | 0.3271 | 20.22 | 1.51 | 0.3247 | 20.80 | 1.39 | 0.3211 | 21.68 |
| | 31 | 1.61 | | | 1.48 | | | 1.36 | | |
| 3 | 10 | 1.54 | 0.3176 | 22.53 | 1.43 | 0.3150 | 23.17 | 1.31 | 0.3110 | 24.15 |
| | 31 | 1.50 | | | 1.39 | | | 1.28 | | |
| | 25 | 0.83 | | | 1.33 | | | 1.22 | | |
| | 18 | 0.59 | | | 0.45 | | | 0.43 | | |
| 4 | 10 | 0.51 | 0.3118 | 23.96 | 0.96 | 0.3089 | 24.65 | 0.91 | 0.3047 | 25.69 |
| | 31 | 1.07 | | | 0.92 | | | 0.87 | | |
| | 25 | 1.03 | | | 0.54 | | | 0.51 | | |
| | 18 | 0.59 | | | 0.44 | | | 0.42 | | |
| | 31 | 1.07 | | | 0.95 | | | 0.90 | | |
| 5 | 10 | 0.50 | 0.3100 | 24.39 | 0.89 | 0.3071 | 25.10 | 0.85 | 0.3028 | 26.16 |
| | 25 | 1.00 | | | 0.89 | | | 0.87 | | |
| | 18 | 0.59 | | | 0.54 | | | 0.51 | | |
| | 22 | 0.52 | | | 0.47 | | | 0.44 | | |
| | 31 | 1.07 | | | 0.95 | | | 0.90 | | |
| 6 | 10 | 0.47 | 0.3090 | 24.63 | 0.42 | 0.3061 | 25.34 | 0.40 | 0.3017 | 26.40 |
| | 31 | 0.80 | | | 0.72 | | | 0.68 | | |
| | 25 | 0.98 | | | 0.88 | | | 0.83 | | |
| | 18 | 0.59 | | | 0.54 | | | 0.51 | | |
| | 22 | 0.52 | | | 0.47 | | | 0.44 | | |
| | 29 | 0.37 | | | 0.57 | | | 0.51 | | |
| | 31 | 1.07 | | | 0.95 | | | 0.90 | | |

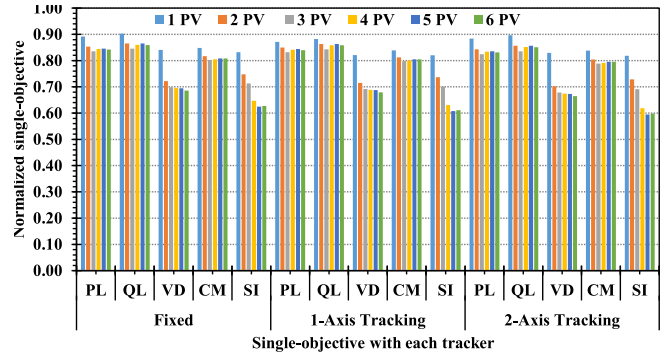


Fig. 3. Single-objective functions for different PV numbers with the three trackers.

Another notice is that the utilization of 2-axis PV trackers can have further benefits in terms of the technical condition of the distribution system with PV. These benefits are quantified in the table where the highest f_{IP} values (i.e., lowest f_{PV}) are noticed with 2-axis PV trackers compared to the other trackers. For example, for the case of 6 PVs, f_{IP} is 26.40% with 2-axis PV trackers which is higher than those of fixed units (24.63%) and 1-axis PV trackers (25.34%). The reason for this difference is that the PV generation profile with 2-axis PV trackers is more regulated than the other trackers, as demonstrated in Fig. 1. However, these further technical benefits of the 2-axis solar tracking systems will be at the expense of their higher capital and maintenance costs compared to the two other tracking systems. Interestingly, the higher the number of PV units to be allocated, the higher the technical benefits to be accomplished in general, but at different rates for the three trackers. Similar to the full objective function, the same conclusion is noticed for the values of the five single-objective functions for different numbers of PV units with different trackers shown in Fig. 3. This trend implies that the selection of PV tracker can have great impacts not only on the optimal PV capacity but also on the diverse technical benefits to distribution systems.

Fig. 4 shows the computed PV size with fixed, 1-axis, and 2-axis PV trackers at each bus (with one PV unit) of the distribution system and the corresponding estimated f_{PV} . To validate

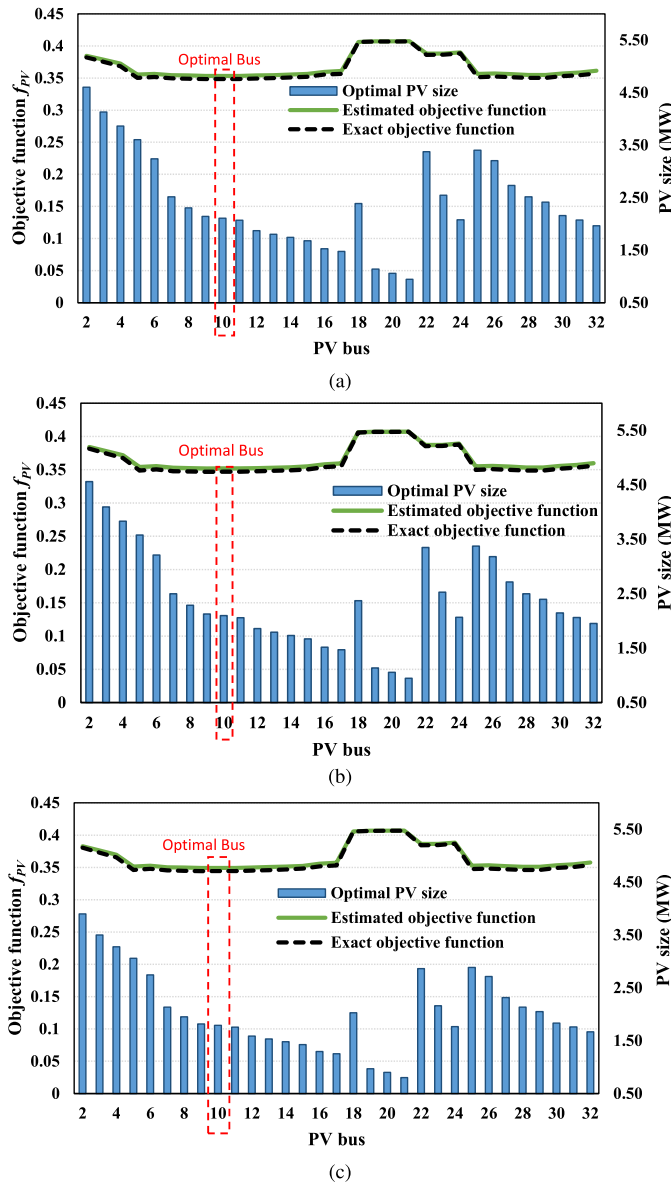


Fig. 4. Optimal PV size at each bus by the proposed method, and the corresponding estimated and exact objective function values. (a) Fixed PV, (b) 1-axis trackers, and (c) 2-axis trackers.

the accuracy of the proposed analytical expressions for f_{PV} assessment with PV, the corresponding exact f_{PV} values computed by power flow analysis are shown in the same figure. It is obvious that the estimated f_{PV} values are strongly matched with its exact values for different PV locations with the three different tracking systems. This strong matching proves the high accuracy rate of the proposed CAEs to calculate optimal solutions. More importantly, their minimum values are attained at the same bus (Bus 10), allowing to identify the optimal bus directly among all valid buses without requiring iterative process.

Regarding the computational performance, the proposed PV planning method is computationally efficient since it is direct. Unlike metaheuristic algorithms which consume several hours due to exhaustive power flow calculations for converging to near-optimal solutions, the computational time of the proposed

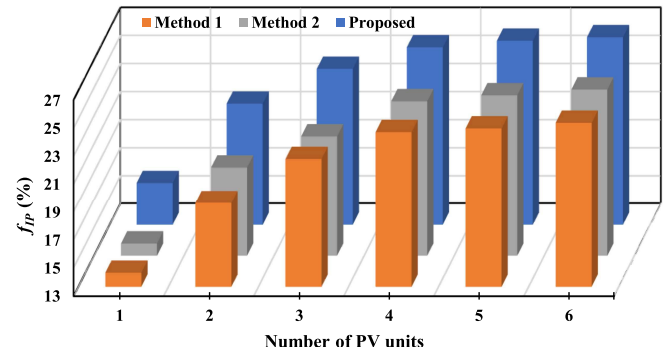


Fig. 5. f_{IP} values in the case of the proposed method, Method 1, and Method 2 with different numbers of PV.

method is relatively very small, thanks to avoiding power flow calculations.

C. Performance Evaluation of CAEs

Fig. 5 compares f_{IP} values in the case of the proposed method and two existing methods (Methods 1 and 2) with different numbers of PV. Method 1 and Method 2 utilize active losses and reactive losses, respectively, as objectives for the PV planning problem. Active losses and reactive losses are considered as objectives in [41] and [37], respectively. For each PV number, the corresponding f_{IP} value in the case of the proposed method is much higher than those of Method 1 and Method 2. This comparison illustrates the effectiveness of the proposed CAEs which utilizes multi-objectives to maximize the benefits of PV to distribution systems compared to single-objective based methods.

Further, the effect of weights for single-objectives on the PV planning problem is demonstrated here. For this purpose, we study the variation of the single-objectives with the setting of a weight factor. Specifically, we solve the PV planning model with different WF_1 values where WF_1 is increased from 0.0 to 1.0 with a step of 0.20. Note that for all values of WF_1 , the values of the other four weights are set to be similar while the sum of all five weights is equal to 1.0. As shown in Fig. 6, PL_{PV} decreases continuously when increasing its weight (WF_1) whereas this reduction is accomplished at the expense of the other four single-objectives. To illustrate this penalty, we show the SI_{PV} at the same figure whose value increases with WF_1 , unlike PL_{PV} . This analysis highlights the flexibility of the proposed expressions that provide distribution system planners the ability to make a trade-off among the conflicting objectives according to adopted regulations by utilities.

D. Effects of the Active Power Curtailment of Smart PV Inverter

Fig. 7 shows the variation of the optimal sizes of 6 PV units computed by the proposed method with the curtailment factor (CF) of the interfacing inverter. CF represents the maximum allowed curtailment amount divided by the nominal capacity. In this experiment, the CF value is increased from

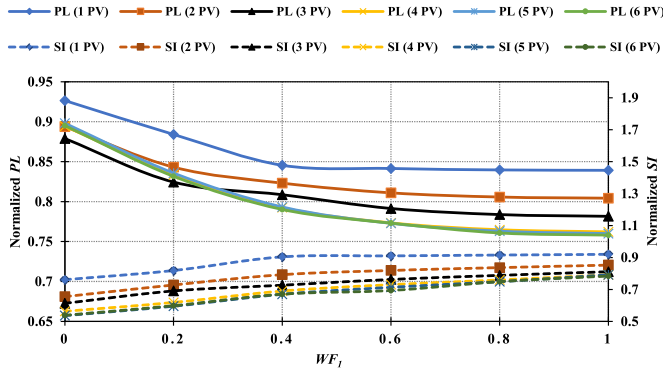


Fig. 6. Effect of increasing WF_1 on two single-objective functions with 1-6 PV units.

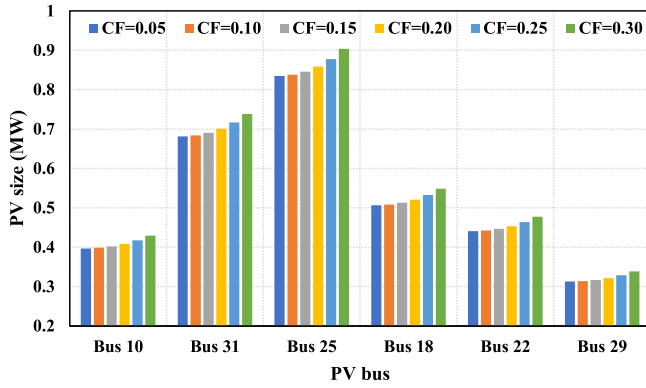


Fig. 7. The variation of the optimal sizes of 6 PV units computed by the proposed method with the curtailment factor (CF) of the interfacing inverter.

0.05 to 0.30 with a step of 0.05. In particular, we have formulated the active power curtailment as a percentage of the nominal capacity of PV arrays. However, the active power curtailment is considered to be applied only when the available PV power is higher than the rating of the interfacing inverter, i.e., the inverter DC-to-AC ratio. Hence, the curtailment period is supposed to be certain hours during the middle of the day, not all the day. It is observed in Fig. 7 that the PV sizes at all buses increase with the CF values while the corresponding objective value is almost kept the same with the different CF values ($f_{PV} = 0.30$). Therefore, it can be concluded that adopting the active power curtailment of PV can extend the allowed PV penetration in distribution systems. This analysis illustrates the flexibility of the proposed method to consider curtailment strategies in the planning phase of PV.

E. Reactive Power Capability of Smart PV Inverter

Here, we compare the impacts of different reactive power-management approaches (Approaches 1, 2, 3, and 4) of the interfacing inverter on the PV planning. Approaches 1 and 2 involve leading and lagging power factor settings, respectively. Approaches 3 and 4 include the default voltage-var setting and the proposed optimized power factor setting, respectively. In Approaches 1 and 2, the inverter operates with constant power factor operation with 0.9 leading and 0.9 lagging power factors. The constraints incorporated for inverter power factor in

Approach 3 is 0.9 leading and 0.9 lagging power factors. In turn, the proposed optimized power factor setting computed the optimal power factor for each state within the power factor ranges of 0.9 leading and 0.9 lagging power factors. The power factor range is 0.9 leading and lagging Fig. 8 shows that the lowest objective function f_{PV} are accomplished by the proposed approach (Approach 4) with different PV numbers. Another benefit is that the computed total PV capacity by Approach 4 is higher than Approaches 1 and 3, allowing to maximize the PV hosting capacity.

F. Application to PV Assessment and Control

In this subsection, we first show the applicability of the proposed formulations to the rapid assessment of PV impacts in a short time. For this purpose, the proposed analytical expressions (11)-(15) are utilized to directly compute the five indices for the distribution system interconnected with up to 6 PV units for annual hourly simulations. Table VI shows the root mean square errors ($E_{PL}, E_{QL}, E_{VD}, E_{CM}, E_{SI}$) between the five indices computed by (11)-(15) with respect to the corresponding exact ones computed by the power flow computational method. As shown, these errors are very small with different numbers of PV units, indicating that the five indices calculated by the proposed analytical expressions strongly match the exact values. This trend reveals the high accuracy rate of the proposed analytical expressions for assessing the impacts of PVs on the distribution system performance. Further, we evaluate the computational performance of the proposed method with the different numbers of PV units in Table VI. As shown, the computational times of the proposed method are very small with the different numbers of PV units (less than 2.0 seconds). The corresponding speedup values of the proposed method respecting to the power flow computational method are above 28. Accordingly, it is clear that the computational burden of proposed analytical expressions is light, allowing to provide fast annual PV assessment results.

The proposed analytical expressions (18) can be also used for the optimal inverter control not only to solve local voltage violations but also to maximize the grid benefits in terms of the five indices in a very fast way. Table VII shows the computational performance of the proposed formulation for the optimal control of the PV inverter per time instance with 1-6 PV units. The computational time for solving the program is 0.4657 ms in the case of 6 PV units where a centralized control action of the 6 inverters is accomplished. However, it is only 0.0372 ms with one PV unit which can represent the case when there is no cooperation among the PV inverters (decentralized control). This feature is accomplished as the proposed analytical expressions are solved directly without requiring iterative processes. The high computational performance and the simplicity of the CAEs make them more amenable to practical real-time implementations.

Accordingly, the proposed analytical expressions are applicable to the fast assessment of PV impacts and to optimal centralized/decentralized PV inverter control. In turn, the optimization-based approaches, which suffer from a heavy

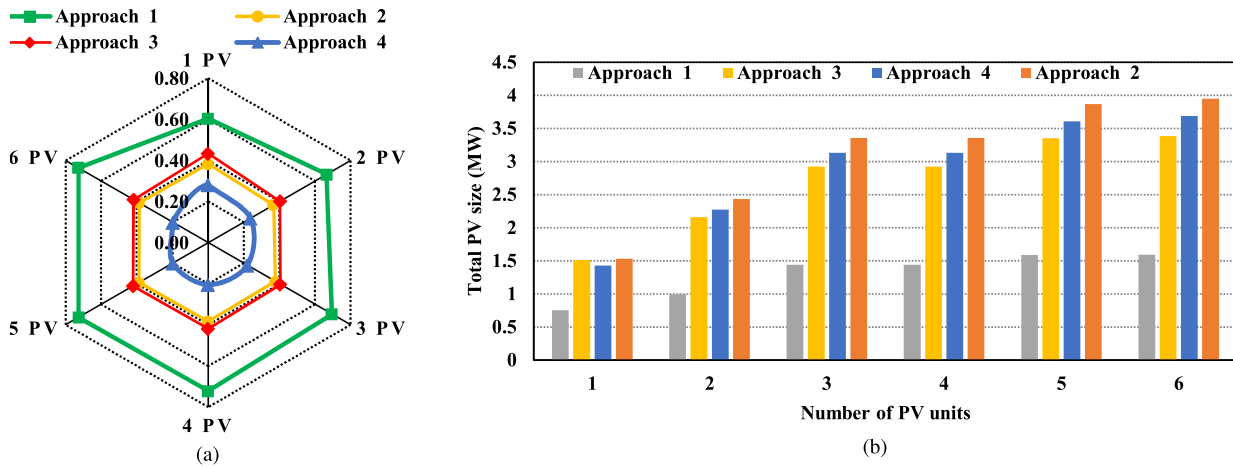


Fig. 8. Results of the PV allocation problem by Approaches 1, 2, 3, and 4. (a) the objective function and (b) total PV size in the distribution system.

TABLE VI
PERFORMANCE OF PROPOSED EXPRESSIONS FOR ANNUAL SIMULATION

| U | 1 | 2 | 3 | 4 | 5 | 6 |
|--------------|--------|--------|--------|--------|--------|--------|
| E_{PL} | 0.0286 | 0.0456 | 0.0469 | 0.0544 | 0.0541 | 0.0540 |
| E_{QL} | 0.0322 | 0.0502 | 0.0504 | 0.0603 | 0.0601 | 0.0594 |
| E_{VD} | 0.0315 | 0.0366 | 0.0360 | 0.0444 | 0.0442 | 0.0429 |
| E_{CM} | 0.0095 | 0.0177 | 0.0197 | 0.0221 | 0.0228 | 0.0233 |
| E_{SI} | 0.0184 | 0.0303 | 0.0318 | 0.0469 | 0.0474 | 0.0461 |
| CPU Time (s) | 1.41 | 1.50 | 1.59 | 1.62 | 1.73 | 1.83 |
| Speedup | 37.34 | 34.96 | 32.99 | 32.45 | 30.41 | 28.78 |

TABLE VII
COMPUTATIONAL PERFORMANCE OF PROPOSED EXPRESSIONS FOR OPTIMAL INVERTER CONTROL

| U | 1 | 2 | 3 | 4 | 5 | 6 |
|---------------|--------|--------|--------|--------|--------|--------|
| CPU Time (ms) | 0.0372 | 0.0881 | 0.1312 | 0.2441 | 0.3413 | 0.4657 |

computational burden, can be appropriate for PV planning; However, their implementation to the PV assessment and control is challenging, especially in real-time control applications. Based on the superior computational performance of the proposed CAEs, they can remove the limitations of allocating and controlling PV units in distribution systems and open the door towards a comprehensive assessment of PV.

It is important to note that the proposed CAEs for assessing and maximizing the technical benefits of photovoltaics are directed to medium-voltage distribution systems, not low-voltage distribution systems. Such concerned medium-voltage distribution systems are commonly modeled as balanced systems in the literature where the unbalance impacts are slight. Nevertheless, the proposed analytical expressions can be utilized to consider the three-phase imbalance in distribution systems by performing the following steps. The first step is to convert three-phase-coupled distribution lines into their equivalent decoupled models as demonstrated in a previous study [46]. The next step is to apply the CAEs for each phase of the resulting decoupled line models. Accordingly, the proposed CAEs can provide the required results planning assessment, control results for each phase complying with the multi-phase distribution systems.

VI. CONCLUSION

In this paper, we have proposed CAEs to maximize the technical benefits of PV units to distribution systems. The proposed CAEs can directly determine the optimal locations and sizes of multiple PV units without needing iterative processes. A multi-objective based PV planning model that comprises five vital indices was formulated considering the uncertainty of PV and load profiles. Another benefit of the proposed CAEs is the consideration of the smart functions of the PV inverter, including reactive power support and active power curtailment. Comprehensive simulations with different scenarios are performed to demonstrate the effectiveness of the proposed CAEs for optimally allocating multiple PV units. The proposed PV planning method was tested on the IEEE 33-bus distribution system considering various TOs (fixed, one-axis, and two-axis trackers). The results demonstrate the accuracy and flexibility of the proposed CAEs which allow to adjust the trade-off between the conflicting single-objectives while adopting the smart functions of the PV inverter in the planning stage. Additionally, the proposed CAEs are a promising tool for the assessment of PV impacts in a short time and the optimal PV inverter control, and so they are suitable for real-time applications.

REFERENCES

- [1] P. H. Divshali and L. Söder, "Improving hosting capacity of rooftop PVs by quadratic control of an LV-central BSS," *IEEE Trans. Smart Grid*, vol. 10, no. 1, pp. 919–927, Jan. 2019.
- [2] M. N. I. Sarkar, L. G. Meegahapola, and M. Datta, "Reactive power management in renewable rich power grids: A review of grid-codes, renewable generators, support devices, control strategies and optimization algorithms," *IEEE Access*, vol. 6, pp. 41458–41489, 2018.
- [3] T. R. Ricciardi, K. Petrou, J. F. Franco, and L. F. Ochoa, "Defining customer export limits in PV-Rich low voltage networks," *IEEE Trans. Power Syst.*, vol. 34, no. 1, pp. 87–97, Jan. 2019.
- [4] S. Hashemi and J. Østergaard, "Efficient control of energy storage for increasing the PV hosting capacity of LV grids," *IEEE Trans. Smart Grid*, vol. 9, no. 3, pp. 2295–2303, May 2018.
- [5] M. Ahmadi, M. E. Lotfy, R. Shigenobu, A. M. Howlader, and T. Senjyu, "Optimal sizing of multiple renewable energy resources and PV inverter reactive power control encompassing environmental, technical, and economic issues," *IEEE Syst. J.*, vol. 13, no. 3, pp. 3026–3037, Sep. 2019.

- [6] B. Singh and B. J. Gyanish, "Impact assessment of DG in distribution systems from minimization of total real power loss viewpoint by using optimal power flow algorithms," *Energy Rep.*, vol. 4, pp. 407–417, Nov. 2018.
- [7] Q. Li, R. Ayyanar, and V. Vittal, "Convex optimization for DES planning and operation in radial distribution systems with high penetration of photovoltaic resources," *IEEE Trans. Sustain. Energy*, vol. 7, no. 3, pp. 985–995, Jul. 2016.
- [8] M. ElNozahy, T. K. Abdel-Galil, and M. M. A. Salama, "Probabilistic ESS sizing and scheduling for improved integration of phev and PV systems in residential distribution systems," *Elect. Power Syst. Res.*, vol. 125, pp. 55–66, Aug. 2015.
- [9] Photovoltaics, Dispersed Generation, and Energy Storage, *IEEE Standard for Interconnection and Interoperability of Distributed Energy Resources With Associated Electric Power Systems Interfaces*, IEEE Standard IEEE 1547-2018, 2018.
- [10] R. A. Jabr, "Robust volt/VAR control with photovoltaics," *IEEE Trans. Power Syst.*, vol. 34, no. 3, pp. 2401–2408, May 2019.
- [11] B. Zhang, P. Dehghanian, and M. Kezunovic, "Optimal allocation of PV generation and battery storage for enhanced resilience," *IEEE Trans. Smart Grid*, vol. 10, no. 1, pp. 535–545, Jan. 2019.
- [12] R. S. Al Abri, E. F. El-Saadany, and Y. M. Atwa, "Optimal placement and sizing method to improve the voltage stability margin in a distribution system using distributed generation," *IEEE Trans. Power Syst.*, vol. 28, no. 1, pp. 326–334, Feb. 2013.
- [13] S. S. Alkaabi, H. H. Zeineldin, and V. Khadkikar, "Short-term reactive power planning to minimize cost of energy losses considering PV systems," *IEEE Trans. Smart Grid*, vol. 10, no. 3, pp. 2923–2935, May 2019.
- [14] S. S. Alkaabi, H. H. Zeineldin, and V. Khadkikar, "Adaptive planning approach for customer DG installations in smart distribution networks," *IET Renew. Power Gener.*, vol. 12, no. 1, pp. 81–89, 2018.
- [15] S. S. AlKaabi, V. Khadkikar, and H. H. Zeineldin, "Incorporating PV inverter control schemes for planning active distribution networks," *IEEE Trans. Sustain. Energy*, vol. 6, no. 4, pp. 1224–1233, Oct. 2015.
- [16] S. Wang, Y. Dong, L. Wu, and B. Yan, "Interval overvoltage risk based PV hosting capacity evaluation considering PV and load uncertainties," *IEEE Trans. Smart Grid*, vol. 11, no. 3, pp. 2709–2721, May 2020.
- [17] M. Z. Liu *et al.*, "On the fairness of PV curtailment schemes in residential distribution networks," *IEEE Trans. Smart Grid*, vol. 11, no. 5, pp. 4502–4512, Sep. 2020.
- [18] M. D. Hraiz, J. A. M. García, R. J. Castañeda, and H. Muhsen, "Optimal PV size and location to reduce active power losses while achieving very high penetration level with improvement in voltage profile using modified Jaya algorithm," *IEEE J. Photovolt.*, vol. 10, no. 4, pp. 1166–1174, Jul. 2020.
- [19] C. K. Das, O. Bass, G. Kothapalli, T. S. Mahmoud, and D. Habibi, "Optimal placement of distributed energy storage systems in distribution networks using artificial bee colony algorithm," *Appl. Energy*, vol. 232, pp. 212–228, Dec. 2018.
- [20] A. Ali, D. Raisz, K. Mahmoud, and M. Lehtonen, "Optimal placement and sizing of uncertain PVs considering stochastic nature of PEVs," *IEEE Trans. Sustain. Energy*, vol. 11, no. 3, pp. 1647–1656, Jul. 2020.
- [21] M. Ahmadi, M. E. Lotfy, R. Shigenobu, A. Yona, and T. Senjyu, "Optimal sizing and placement of rooftop solar photovoltaic at Kabul city real distribution network," *IET Gener. Transm. Distrib.*, vol. 12, no. 2, pp. 303–309, 2018.
- [22] J. Radosavljević, N. Arsić, M. Milovanović, and A. Ktena, "Optimal placement and sizing of renewable distributed generation using hybrid metaheuristic algorithm," *J. Mod. Power Syst. Clean Energy*, vol. 8, no. 3, pp. 499–510, May 2020.
- [23] O. Erdinç, A. Taşçıkaraoğlu, N. G. Paterakis, I. Dursun, M. C. Sinim, and J. P. S. Catalão, "Comprehensive optimization model for sizing and siting of DG units, EV charging stations, and energy storage systems," *IEEE Trans. Smart Grid*, vol. 9, no. 4, pp. 3871–3882, Jul. 2018.
- [24] C. D. Rodríguez-Gallegos *et al.*, "A siting and sizing optimization approach for PV–battery–diesel hybrid systems," *IEEE Trans. Ind. Appl.*, vol. 54, no. 3, pp. 2637–2645, May/Jun. 2018.
- [25] M. J. E. Alam, K. M. Muttaqi, and D. Sutanto, "Community energy storage for neutral voltage rise mitigation in four-wire multigrounded LV feeders with unbalanced solar PV allocation," *IEEE Trans. Smart Grid*, vol. 6, no. 6, pp. 2845–2855, Nov. 2015.
- [26] S. M. Hakimi, A. Hasankhani, M. Shafie-Khah, and J. P. Catalão, "Optimal sizing and siting of smart microgrid components under high renewables penetration considering demand response," *IET Renew. Power Gener.*, vol. 13, no. 10, pp. 1809–1822, 2019.
- [27] H. B. Tolabi, M. H. Ali, and M. Rizwan, "Simultaneous reconfiguration, optimal placement of DSTATCOM, and photovoltaic array in a distribution system based on fuzzy-ACO approach," *IEEE Trans. Sustain. Energy*, vol. 6, no. 1, pp. 210–218, Jan. 2015.
- [28] S. Montoya-Bueno, J. I. Muoz, and J. Contreras, "A stochastic investment model for renewable generation in distribution systems," *IEEE Trans. Sustain. Energy*, vol. 6, no. 4, pp. 1466–1474, Oct. 2015.
- [29] S. Jothibasu, A. Dubey, and S. Santoso, "Two-stage distribution circuit design framework for high levels of photovoltaic generation," *IEEE Trans. Power Syst.*, vol. 34, no. 6, pp. 5217–5226, Nov. 2019.
- [30] X. Xu, J. Li, Y. Xu, Z. Xu, and C. S. Lai, "A two-stage game-theoretic method for residential PV panels planning considering energy sharing mechanism," *IEEE Trans. Power Syst.*, vol. 35, no. 5, pp. 3562–3573, Sep. 2020.
- [31] S. R. K. Najafabadi, B. Fani, and I. Sadeghkhan, "Optimal determination of photovoltaic penetration level considering protection coordination," *IEEE Syst. J.*, early access, Feb. 8, 2021, doi: [10.1109/JSYST.2021.3052527](https://doi.org/10.1109/JSYST.2021.3052527).
- [32] S. F. Santos, D. Z. Fitiwi, M. Shafie-Khah, A. W. Bizuayehu, C. M. P. Cabrita, and J. P. S. Catalão, "New multistage and stochastic mathematical model for maximizing res hosting capacity—Part I: Problem formulation," *IEEE Trans. Sustain. Energy*, vol. 8, no. 1, pp. 304–319, Jan. 2017.
- [33] Z. Abdmouleh, A. Gastli, L. Ben-Brahim, M. Haouari, and N. A. Al-Emadi, "Review of optimization techniques applied for the integration of distributed generation from renewable energy sources," *Renew. Energy*, vol. 113, pp. 266–280, Dec. 2017.
- [34] S. Elsaiah, M. Benidris, and J. Mitra, "Analytical approach for placement and sizing of distributed generation on distribution systems," *IET Gener. Transm. Distrib.*, vol. 8, no. 6, pp. 1039–1049, 2014.
- [35] K. Mahmoud, N. Yorino, and A. Ahmed, "Optimal distributed generation allocation in distribution systems for loss minimization," *IEEE Trans. Power Syst.*, vol. 31, no. 2, pp. 960–969, Mar. 2016.
- [36] D. Q. Hung and N. Mithulananthan, "Multiple distributed generator placement in primary distribution networks for loss reduction," *IEEE Trans. Ind. Electron.*, vol. 60, no. 4, pp. 1700–1708, Apr. 2013.
- [37] K. Mahmoud and M. Lehtonen, "Simultaneous allocation of multi-type distributed generations and capacitors using generic analytical expressions," *IEEE Access*, vol. 7, pp. 182701–182710, 2019.
- [38] H. Khan and M. A. Choudhry, "Implementation of distributed generation (IDG) algorithm for performance enhancement of distribution feeder under extreme load growth," *Int. J. Elect. Power Energy Syst.*, vol. 32, no. 9, pp. 985–997, 2010.
- [39] M. M. Aman, G. B. Jasmon, H. Mokhlis, and A. H. A. Bakar, "Optimal placement and sizing of a DG based on a new power stability index and line losses," *Int. J. Elect. Power Energy Syst.*, vol. 43, no. 1, pp. 1296–1304, 2012.
- [40] D. Q. Hung and N. Mithulananthan, "Loss reduction and loadability enhancement with DG: A dual-index analytical approach," *Appl. Energy*, vol. 115, pp. 233–241, Feb. 2014.
- [41] D. Q. Hung, N. Mithulananthan, and K. Y. Lee, "Determining PV penetration for distribution systems with time-varying load models," *IEEE Trans. Power Syst.*, vol. 29, no. 6, pp. 3048–3057, Nov. 2014.
- [42] K. Mahmoud, N. Yorino, and A. Ahmed, "Power loss minimization in distribution systems using multiple distributed generations," *IEEE Trans. Elect. Electron. Eng.*, vol. 10, no. 5, pp. 521–526, 2015.
- [43] H. Chen, J. Chen, D. Shi, and X. Duan, "Power flow study and voltage stability analysis for distribution systems with distributed generation," in *Proc. IEEE Power Eng. Soc. Gen. Meeting*, Montreal, QC, Canada, 2006, p. 8.
- [44] A. R. Bergen and V. Vittal, *Power Systems Analysis*. Englewood Cliffs, NJ, USA: Prentice-Hall, 2009.
- [45] *NREL's PVWatts® Calculator*. Accessed: Mar. 1, 2021. [Online]. Available: <https://pvwatts.nrel.gov/index.php>
- [46] K. Mahmoud and N. Yorino, "Robust quadratic-based BFS power flow method for multi-phase distribution systems," *IET Gener. Transm. Distrib.*, vol. 10, no. 9, pp. 2240–2250, 2016.



Karar Mahmoud received the B.Sc. and M.Sc. degrees in electrical engineering from Aswan University, Aswan, Egypt, in 2008 and 2012, respectively, and the Ph.D. degree from the Electric Power and Energy System Laboratory, Graduate School of Engineering, Hiroshima University, Hiroshima, Japan, in 2016.

Since 2010, he has been with Aswan University, where he is currently an Associate Professor with the Electrical Engineering Department. He is currently a Postdoctoral Researcher with Prof. M. Lehtonen's

Group, School of Electrical Engineering, Aalto University, Finland. He has authored or coauthored several publications in top-ranked journals including IEEE journals, international conferences, and book chapters. His research interests include power systems, renewable energy sources, smart grids, distributed generation, optimization, applied machine learning, IoT, industry 4.0, and high voltage. In 2021, he becomes a Topic Editor in *Sensors* (MDPI).



Matti Lehtonen received the master's and Licentiate degrees in electrical engineering from the Helsinki University of Technology, Finland, in 1984 and 1989, respectively, and the Doctor of Technology degree from the Tampere University of Technology, Finland, in 1992. He was with VTT Energy, Espoo, Finland, from 1987 to 2003, and since 1999, has been a Full Professor and the Head of the Power Systems and High Voltage Engineering Group, Aalto University, Espoo, Finland. His research interests include power system planning and assets management, power system protection, including earth fault problems, harmonic related issues, power cable insulation, and polymer nanocomposites. He is an Associate Editor for *Electric Power Systems Research* and *IET Generation, Transmission Distribution*.